analytical chemistry

Article

pubs.acs.org/ac

Real-Time Study of Interactions between Cytosine–Cytosine Pairs in DNA Oligonucleotides and Silver Ions Using Dual Polarization Interferometry

Yu Zheng,[†,‡] Cheng Yang,[†,‡] Fan Yang,*[,†] and Xiurong Yang*[,†]

[†]State Key Laboratory of Electroanalytical Chemistry, Changchun Institute of Applied Chemistry, Chinese Academy of Sciences, Changchun, Jilin 130022, China

[‡]University of Chinese Academy of Sciences, Beijing 100039, China

Supporting Information

ABSTRACT: The real-time conformational changes of cytosine (C)-rich ssDNA oligonucleotides upon binding with silver ions (Ag^+) were studied using dual polarization interferometry (DPI). Upon the addition of Ag^+, Ag^+ selectively bound to cytosine–cytosine mismatches and formed C–Ag^+–C complexes, inducing change of the structure of the C-rich ssDNA from random coil conformation to duplex conformation, whereas the control ssDNA without cytosine–cytosine mismatches had no such signal, which was consistent with circular dichroism (CD) characterization. The conformational change of DNA was reflected on the changes of the mass, thickness, and density values resolved by DPI. The calibration curves showed that as the concentration of Ag^+ increased from 10 nM to 8 μM, the thickness and mass values increased linearly while the density values decreased linearly. Other metal ions such as K^+, Ca^{2+}, Na^+, Mg^{2+}, Zn^{2+}, Mn^{2+}, Ni^{2+}, and Pb^{2+} did not interfere with the interaction between Ag^+ and C-rich ssDNA, indicating that this method had a good selectivity. The practical application of this biosensor was also investigated in real samples such as drinking water. Besides, cysteine could specifically capture Ag^+ from C–Ag^+–C complexes and transformed the structure of the C-rich DNA back from rigid double-stranded conformation to random coil conformation, which allowed cysteine to be detected selectively as well. It is expected that this biosensing strategy may be utilized to study the interaction of DNA with other molecules.

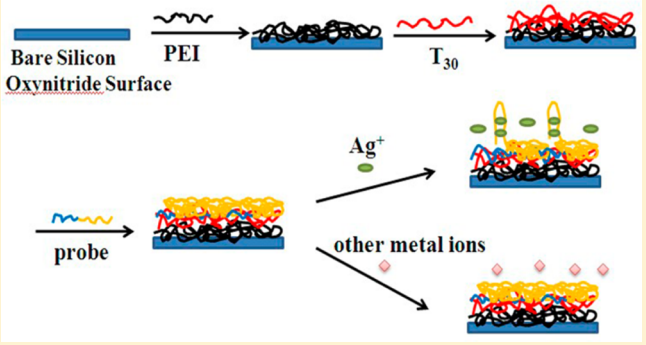

Silver has been used in various applications such as in food, water purification, and medical materials for a long time because it inhibits activities of many bacteria, viruses, and cancer cells.[1−5] However, silver ion also does harm to the environment and the human body as a heavy metal ion. It is highly toxic to aquatic life[6,7] and may destroy the aquatic ecosystems.[8] As Ag^+ could bind to many metabolites and inactivate sulfhydryl enzymes, it may produce dose-dependent cytopathogenic effects in distinct cell types.[9,10] Besides, Ag^+ can selectively bind to cytosine–cytosine (C–C) mismatches and forms C–Ag^+–C complexes in DNA duplexes,[11−14] which may interfere in the replication and transcription of DNA. Thus, it is of great importance to study the interaction of Ag^+ with DNA and develop highly sensitive detection method for Ag^+. Very recently, a variety of methods[15−23] have been used to study the interaction of Ag^+ with DNA, including colorimetric,[16,19] fluorescent,[20,23] luminescent,[21] and so forth. However, most of these techniques could not simultaneously provide real-time structural and kinetic information and thus could not describe DNA conformational change and the interaction of Ag^+ with DNA in detail.

Dual polarization interferometry (DPI) is an effective optical analytical method for real-time and quantitative analysis of the adsorption of biomolecules on interfaces[24] or to study the interaction of biomolecules on the surface with molecules in solution.[25,26] In the past years, DPI has been utilized to monitor protein adsorption,[27−40] polyelectrolyte assembly,[41−45] lipid membrane formation,[46−51] the dynamic interaction of protein with ligands,[52−55] DNA oligonucleotide hybridization,[56−59] among others. Every slight change in the solution would lead to the change of the sensing interface. It is known that electrochemical quartz crystal microbalance (EQCM) has been a well-established analytical technique for the investigation of mass changes on the reactive surface,[60−62] whereas the mass sensitivity of DPI (0.1 pg/mm^2)[63] is much higher than that of EQCM (50 pg/mm^2).[62] Besides, EQCM could only give the information of interfacial mass and charge changes, and DPI could also monitor the thickness and density changes of the

Received: December 10, 2013
Accepted: March 11, 2014
Published: March 11, 2014

interface. Thus, in recent years, the use of DPI to study the interaction of DNA with small molecules has attracted more and more attention. Özalp immobilized the aptamer of argininamide on the silicone oxynitride sensor surfacem, determined the interaction of argininamide with its aptamer, and quantified argininamide according to the conformation change of the aptamer using DPI.[64] Our group utilized DPI for real-time study of genomic DNA structural changes upon interaction with small molecules such as ethidium bromide (EtBr),[65] spermine,[65] mitoxantrone (MTX),[66] and methylene blue (MB)[66], and we probed the interaction of mercury(II)[67] with their respective specific DNA sequences. Actually, the DNA immobilization onto substrate surfaces has been utilized in many areas such as gene delivery, diagnostics, drug development, molecule detection, and so on.[68−70] Because it is well-known that many factors like pH, salt concentration, and temperature affect the conformation of DNA, DNA of the same sequence may have numerous conformations. As different conformations may work oppositely, the real-time control and observation of DNA structural or conformational change at all times is a key factor to precisely understand the interaction of DNA with other molecules and thereby exploit more DNA-related products. DPI, as an effective analytical technique, not only gives a simple sensor response function out but also provides both kinetic and structural information in real time, through which we could "see" the whole process of the conformational change of the DNA. Consequently, DPI is a good candidate to study the interaction between DNA and small molecules in real time.

In this work, we applied the DPI technique to detect the interaction of the heavy metal ion Ag^+ with cytosine (C)-rich ssDNA. The C-rich sequences were immobilized on the surface of the sensing chip. Ag^+ in the solution was flowed over the chip and selectively bound to cytosine−cytosine (C−C) mismatches strongly, forming C−Ag^+−C complexes, which transformed the cytosine-rich DNA structure from random coil conformation to double-stranded conformation. The conformational change of the DNA on the interface upon interacting with Ag^+ caused the changes of the TE phase and TM phase. Both TE and TM phase were analyzed and converted to real-time refractive index, thickness, mass, and density values. The experiment results showed that the changes of the refractive index, thickness, mass, and density values were proportional to the concentration of Ag^+ in the solution respectively. This proved that our strategy could be a good alternative for selective and sensitive determination of Ag^+. Besides, cysteine has a strong reaction with Ag^+ and it could capture Ag^+ from C−Ag^+−C complexes,[71−73] thus, cysteine could also be detected.

EXPERIMENTAL SECTION

Materials. Poly (ethylenimine) (PEI, MW. 25000) was obtained from Sigma -Aldrich (St Louis, MO). Tris (hydroxymethyl) aminomethane (Tris) was obtained from a brand of EMD Biosciences, Inc. (La Jolla, CA, Germany). Perchloric acid ($HClO_4$), sodium perchlorate monohydrate ($NaClO_4·H_2O$), silver nitrate ($AgNO_3$), and other metal ions were purchased from Beijing Chemical Reagent Co. (Beijing, China). Cysteine and other amino acids were purchased from Beijing Dingguo Biotechnology Co. (Beijing, China). Ultrapure water (Milli-Q synthesis, Millipore, Inc., Bedford, MA) was used throughout. Tris-$HClO_4$ buffer solution was prepared with 10 mM Tris-$HClO_4$ and 200 mM $NaClO_4$. The buffer solution was filtered and degassed before use. Homothymine (30-mer) ssDNA oligonucleotides (T_{30}), 49-mer cytosine-rich ssDNA oligonucleotides containing silver-specific sequences (probe: 5′-AAA AAA AAA AAA AAA TTT TCC CCC CCC CCC CCT TTT CCG CCG CCG CCG C-3′), and 49-mer oligonucleotides without silver-specific sequences (control DNA: 5′-AAA AAA AAA AAA AAA TTT TAG ATG TTA TTT TAG ATG TAT TTT AGT TAG T-3′) employed in this experiment were synthesized by Sangon Biotechnology Co. Ltd. (Shanghai, China). Before use, oligonucleotides were dissolved in ultrapure water as stock solutions, and the concentrations were quantified by measuring the UV absorption at 260 nm. The stock solutions were stored in a refrigerator at 4 °C before use. A 10 mM stock solution of $AgNO_3$ was prepared in ultrapure water and kept from light at 4 °C. All chemicals were of analytical grade and used without further purification or treatment. Unless otherwise mentioned, all work solutions were prepared with Tris-$HClO_4$ buffer solution (10 mM, pH 7.0, 200 mM $NaClO_4$).

DPI Experiments. DNA immobilization and interaction with Ag^+ were monitored in real time utilizing a DPI instrument (AnaLight Bio200, Farfield Group Ltd., Crewe, U.K.). Unmodified silicon oxynitride AnaChip (FB 80, Farfield Scientific Ltd.) was used for all experiments. Before use, the chip was first cleaned with Piranha solution (a 7:3 mixture of concentrated sulfuric acid and 30% hydrogen peroxide) for 3 h. Subsquently, it was rinsed in ultrapure water under sonication four times (6 min each time) and then dried under a stream of nitrogen to get rid of water from the surface.

All experiments were performed at 20 ± 0.002 °C in 10 mM Tris-$HClO_4$ running buffer solution (pH 7.0, 200 mM $NaClO_4$). After the cleaned chip was loaded into the instrument, the running buffer solution was passed over the chip at a flow rate of 50 μL/min. When the baseline was stable, an 80% (v/v) ethanol/water solution and ultrapure water with known refractive indexes were sequentially injected into the two channels to calibrate the chip and the running buffer. Thickness and refractive index of the top waveguide layer and the refractive index of the running buffer were obtained and applied for the following experiment data calculation.

After calibration, the flow rate of the buffer solution was set at 50 μL/min when the baseline was stable, a PEI (0.003 mg/mL) solution was injected into the two channels for 4 min and incubated for 5 min, and then the flow was returned to the running buffer to stabilize the baseline. Subsequently, 12 μM T_{30} was injected for 4 min and incubated for 5 min, then the flow returned to the running buffer, and when the stable baseline was reached, 5 μM probe or control DNA was injected for 4 min and incubated for 5 min. The running buffer flowed over the chip until the stable baseline was attained. To interrogate the interaction of the probe with Ag^+, Ag^+ solutions with different concentrations ranging from 10 nM to 10 μM were injected, respectively, into the channels for 4 min. To detect cysteine, various concentrations of cysteine were mixed and reacted with 10 μM Ag^+ first for 30 min, respectively, to ensure the formation of Ag^+−cysteine complexes, and the mixtures were injected for 4 min.

All the data measured were analyzed by the analysis software of the AnaLight Bio200 instrument and translated into refractive index, thickness, mass, and density values.

Circular Dichroism (CD) Experiments. CD spectral measurement was performed on a Jasco J-820 circular dichroism spectropolarimeter (Tokyo, Japan). Prior to

measurement, the buffer solution (10 mM Tris-$HClO_4$, pH 7.0, 200 mM $NaClO_4$) was scanned as the background, which would be automatically subtracted from the following CD data. Four hundred microliters of 10 mM Tris-$HClO_4$ buffer solution (pH 7.0, 200 mM $NaClO_4$) containing 2 μM ssDNA (probe or control DNA) was mixed with different concentrations of Ag^+ (0−6 μM) respectively. The mixtures were equilibrated for 5 min at room temperature and then were independently added into a cell made of quartz suprasil (10 mm path length, 0.7 mL volume). The CD spectra were measured at room temperature over the wavelength range of 210−350 nm with a scanning speed of 200 nm per minute. The ultimate reported spectrum was the average of three successive scans.

RESULTS AND DISCUSSION

Immobilization of ssDNA Measured by DPI. In order to study the interaction of C-rich ssDNA with silver ions by DPI, the immobilization of ssDNA on the chip surface was the first and very important step. To create the probe surface, our group previously[65−67] used the electrostatic immobilization approach to adsorb the probes directly onto the PEI layer. However, this approach had a drawback that the electrostatic interaction between ssDNA and PEI was too strong and the flexibility of the immobilized ssDNA was limited, which severely affected the interaction of ssDNA with small molecules. It was reported that PEI layer had little influence on ssDNA as the layers increased, and oligonucleotides in the surface layer were oriented in an intermediate state between verticality and horizontality.[58] Herein, we developed a new immobilization approach based on the previous method. As displayed in Scheme 1, the unmodified silicon oxynitride chip surface was

Scheme 1. Fabrication Process of Biosensing Interface and Detection of Ag^+ Using DPI Technique

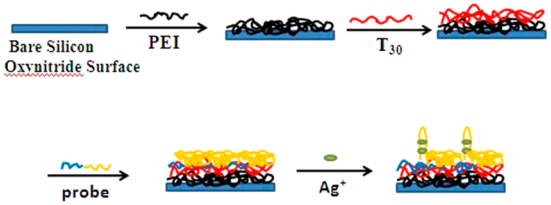

negatively charged at neural pH, hence PEI, which is a cationic polymer, could be deposited on the chip surface, providing a positively charged surface. Then, negatively charged T_{30} was adsorbed electrostatically onto the positively charged PEI, forming a T_{30} layer. Probes or control DNA oligonucleotides containing 15-mer homoadenine sequences (A_{15}) were partially complementary to T_{30} oligonucleotides and thus could hybridize with the T_{30} layer, leading to the successful construction of a functional film.

Figure 1 displayed the real-time measurements of the mass, thickness, and density values for the ssDNA immobilization process. As can be noticed in Figure 1A,B, the initial adsorption of PEI was quick, during which the mass and thickness increased very fast while the density (proportional to refractive index) decreased accordingly. The rate of adsorption slowed down suddenly, and the adsorption of PEI reached a nearly saturated state. Subsequently, the mass, thickness, and density slowly stabilized, during which period the mass of PEI layer remained almost unchanged, and thickness values slightly decreased while the density increased, indicating that the

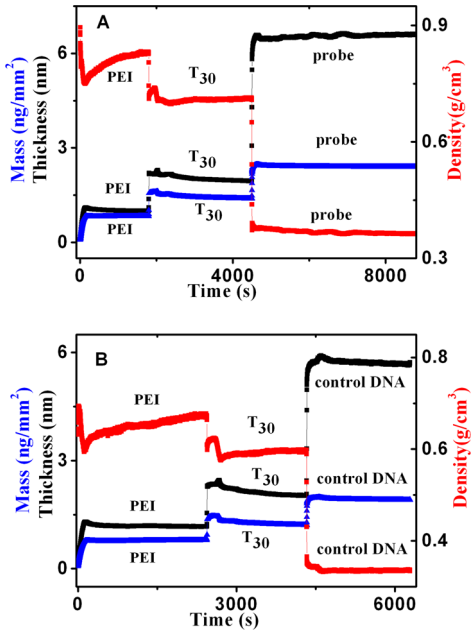

Figure 1. (A) DPI-based real-time measurements of mass (blue triangles), thickness (black squares), and density (red squares) for the whole process of immobilization of PEI, T_{30}, and the probe on the bare silicon oxynitride surface. (B) Real-time DPI measurements of mass (blue triangles), thickness (black squares), and density (red squares) for the whole process of immobilization of PEI, T_{30}, and the control DNA on the bare silicon oxynitride surface.

immobilized PEI layer underwent a conformational rearrangement. When T_{30} was injected, the mass and thickness increased, and the density decreased all at a rapid rate at the beginning, suggesting that T_{30} was deposited quickly. After that, the mass and thickness showed a slight decay with almost the same rate while the density slowly increased, indicating a more compact T_{30} layer. When the buffer was reintroduced to the surface, a desorption process was observed, during which the mass, thickness, and density decreased slowly to stable values, suggesting the structural and conformational rearrangement of T_{30}. As both the probe and control DNA had a 15-mer homoadenine sequence, they were deposited onto the surface by hybridizing with T_{30}. From Figure 1A,B, it is noted that the probe and control DNA adsorption processes were similar to that of T_{30} but with greater changes in the thickness and density value.

The thickness, mass and density values for the stable probe/T_{30}/PEI or control DNA/T_{30}/PEI layer are presented in Table 1. Table 1 shows that DNA layers had lower densities and were more water-swollen than PEI layers, which was consistent with the results of our group's previous work.[65−67] However, the probe or control DNA layer was much thicker and less dense than the T_{30} layer. The thickness of the T_{30} layer was around 0.6 nm, whereas it was about 3−4 nm thick for the probe or control DNA layer from Table 1. It is reported that a DNA strand is about 1.9 nm wide[74] and the average length of the four bases in ssDNA was approximately 0.63 nm,[75] thus the lengths of T_{30} and the probe or control DNA with or without the A_{15} sequence were calculated to be 18.90 nm, 30.87, and 21.42 nm. The thickness value of the T_{30} layer was less than the width value of DNA, indicating that T_{30} molecules were likely to lie on the PEI surface and insert themselves partly into the PEI layer. If the probe or control DNA deposited on the surface

dx.doi.org/10.1021/ac403992r | Anal. Chem. 2014, 86, 3849−3855

Table 1. Layer Structure for probe/T_{30}/PEI or Control DNA/T_{30}/PEI (Mean ± SD, n = 5)

layer material	mass (ng/mm^2)	thickness (nm)	density (g/cm^3)
PEI	0.794 ± 0.067	1.086 ± 0.078	0.733 ± 0.076
T_{30}/PEI	1.239 ± 0.179[a]	1.694 ± 0.175[a]	0.730 ± 0.060[a]
probe/T_{30}/PEI	2.183 ± 0.327[a]	5.517 ± 0.649[a]	0.397 ± 0.057[a]
PEI	0.780 ± 0.021	1.157 ± 0.041	0.674 ± 0.005
T_{30}/PEI	1.066 ± 0.130[a]	1.683 ± 0.304[a]	0.637 ± 0.035[a]
control/T_{30}/PEI	1.640 ± 0.237[a]	4.363 ± 1.150[a]	0.383 ± 0.041[a]

[a]Mass, thickness, and density of the whole T_{30}/PEI, probe/T_{30}/PEI, or control DNA/T_{30}/PEI layer.

oriented either extremely horizontally or extremely vertically, the thicknesses of this layer should be 1.9 or 21.42 nm, respectively. However, the thickness value was around 3 nm for both the probe layer and control DNA layer, which was between 1.9 and 21.42 nm, suggesting that the probe or control DNA might be coiled and oriented in an intermediate state between verticality and horizontality. Besides, this functional layer had a much smaller density than the T_{30} layer, indicating that the probe or control DNA was highly water-swollen with little steric hindrance and received little influence from PEI according to a previous report.[58]

Ag$^+$−DNA Interaction. The functional probe layer was fabricated to study the interaction of silver ions with cytosine-rich ssDNA. As is observed in Scheme 1, Ag$^+$ solution with different concentrations ranging from 10 nM to 10 μM were injected and flowed over the probe layer surface respectively. The probe adsorbed on the interface was of random coil conformation and oriented inclined. When Ag$^+$ was added, it selectively bound to C−C mismatches and formed C−Ag$^+$-C complexes, which transferred the probe structure from flexible single-stranded conformation to rigid duplex conformation. The corresponding real-time thickness, mass and density value changes were presented in Figure 2. It was ever reported that single-stranded DNA oligonucleotides immobilized on the solid surface were flexible with small persistence lengths while double-stranded DNA oligonucleotides were rigid with larger persistence lengths in Tris buffer,[76] thus dsDNA could form a thicker but looser layer than ssDNA. As can be noticed in Figure 2, after the addition of Ag$^+$, the mass and thickness of the layer increased quickly and the density decreased quickly before reaching a equilibrium. When the flow returned to the buffer, the thickness and mass decreased while the density increased, and eventually reached stable values, suggesting the partial dissociation of the probe-Ag$^+$ complexes. Moreover, the changes of the thickness, mass and density values were proportional to the concentration of Ag$^+$ in the range of 10 nM to 8 μM. When the concentration was higher than 8 μM, the binding of Ag$^+$ slowed down, this may be due to the occupation of most of the binding sites in the probe layer.

On the basis of these phenomena, a biosensor for determination of Ag$^+$ was fabricated. As is depicted in Figure S1, the changes of the mass (Figure S1A), thickness (Figure S1B), and density (Figure S1C) value at 450 s were linearly related to the concentration of Ag$^+$ ranging from 10 nM to 8 μM, and the linear equation could be fitted as mass (ng/mm^2) = 0.0012 + 0.00382c (Ag$^+$, μM) (R^2 = 0.991), thickness (nm) = 0.03129 + 0.05453c (Ag$^+$, μM) (R^2 = 0.993), and density (g/cm^3) = −0.00263 − 0.00564c (Ag$^+$, μM) (R^2 = 0.988), respectively. The limits of detection (3σ) were 5 nM for mass calibration, 1 nM for thickness calibration, and 10 nM for density calibration, which were much lower than the maximum

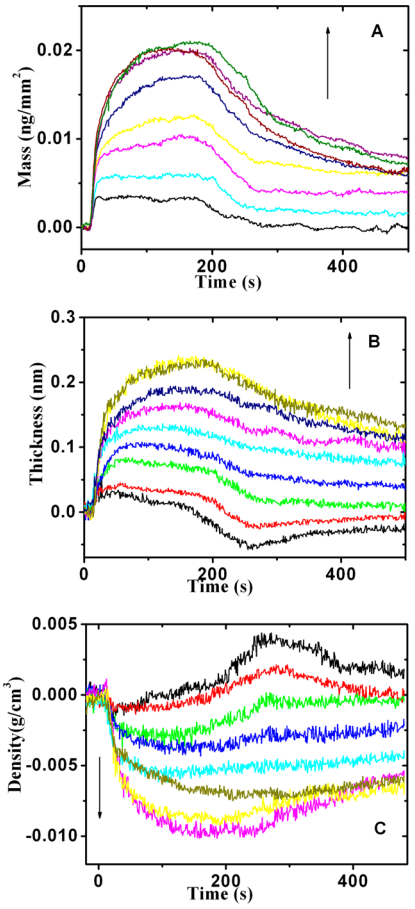

Figure 2. Real-time mass (A), thickness (B), and density (C) value changes of the probe/T_{30}/PEI layer upon Ag$^+$ injection. The arrows show increasing Ag$^+$ concentration.

contaminant level of Ag$^+$ (0.46 μM) in drinking water regulated by World Health Organization (WHO).

To test the practicality of this biosensor, we further detected drinking water as a real sample. To prepare the real samples, 10 μL of drinking water diluted with 590 μL of Tris-$HClO_4$ buffer solution (10 mM, pH 7.0, 200 mM $NaClO_4$) were added with known amounts of Ag$^+$. Results were presented in Table S1, which indicated that the concentration of Ag$^+$ measured was in general accord with that added, and the recoveries calculated from the thickness data were in the range of 88% to 110%, demonstrating that the biosensor had a potential for detecting Ag$^+$ in real samples.

Advantages of the New Method for Immobilizing the Probe. To compare the flexibility of the probe immobilized using this approach (Method A) with the method our group previously[65−67] used (Method B), the probe was then immobilized directly onto the PEI forming probe/PEI layer

dx.doi.org/10.1021/ac403992r | Anal. Chem. 2014, 86, 3849−3855

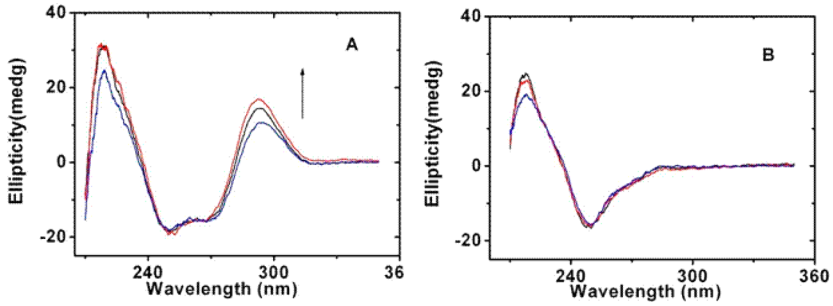

Figure 3. CD spectra of the probe (A) and control DNA (B) after the addition of different concentrations of Ag^+ in 10 mM Tris-$HClO_4$ buffer solution (pH 7.0, 200 mM $NaClO_4$). The concentration of the probe and the control DNA is 2 μM, the concentrations of Ag^+ are 0 μM, 3 μM, and 6 μM. The arrow shows increasing Ag^+ concentration.

under the same condition as Method A. As depicted in Figure S2, after the addition of Ag^+, the differences of the mass changes (Figure S2A) between these two methods were minimal; however, the thickness (Figure S2B) and density changes (Figure S2C) of Method A were much more sensitive than that of Method B, which indicated that the probe immobilized using Method A underwent a much more sensitive conformational change. These results demonstrated that Method A for creating the probe layer used herein improved the flexibility of the ssDNA and the sensitivity of detecting Ag^+. Besides, the detection limit for Method A was 30 times lower than that for Method B. For Method A, the sensitivity obtained by analysis of the thickness change was much higher than that obtained by analysis of the mass change, and the limits of detection according to thickness was lower than that according to mass, suggesting that thickness change, instead of mass change, became the more convincing element to study the interaction between DNA and Ag^+. Thus, the method we newly developed was a major improvement in fabrication of the DNA-sensing surface, because of which the study of DNA conformational change in real time would be more precise and reliable.

Specificity and Selectivity of Ag^+–DNA Interaction. In order to study the specific binding between C-rich ssDNA and Ag^+, a control experiment was performed using the control DNA instead of the probe. As can be observed in Figure S1, compared to the probe/T_{30}/PEI layer, the control DNA/T_{30}/PEI layer underwent small mass (Figure S1A), thickness (Figure S1B), and density (Figure S1C) changes upon addition of different concentrations of Ag^+, indicating the highly specific binding of Ag^+ toward the C-rich ssDNA.

Besides, other metal ions such as K^+, Ca^{2+}, Na^+, Mg^{2+}, Zn^{2+}, Mn^{2+}, Ni^{2+}, and Pb^{2+} were investigated instead of Ag^+ to study the selectivity of this biosensor for Ag^+. As is shown in Figure S3, the changes of the mass (Figure S3A), thickness (Figure S3B), and density (Figure S3C) values of these metals were much less than that of Ag^+, indicating the high selectivity of this biosensor against Ag^+.

Circular Dichroism Spectroscopy Characterization of Ag^+–DNA Interaction. To further demonstrate the specific interaction of C-rich ssDNA with Ag^+, circular dichroism spectroscopy (CD) of the probe and control DNA before and after binding to Ag^+ was recorded. Figure 3A shows that the probe showed a CD spectrum with a positive ellipticity maximum around 290 nm, two negative minimums around 248 and 270 nm, and a larger positive maximum around 218 nm. According to previous reports,[77,78] a C-rich ssDNA dissolved in neutral buffer possessed a CD spectrum of a positive maximum around 290 nm, a negative minimum around 248 and 270 nm, and a small positive maximum around 218 nm, whereas an A-rich ssDNA possessed a CD spectrum of a negative minimum around 248 nm and a large positive maximum around 218 nm.[79] It could be concluded that the measured CD spectra of the probe were the combination of that of the C-rich ssDNA sequence and the poly(A) sequence. As it was also reported[80] that a hairpin structure possessed a CD spectrum characterized by a positive ellipticity maximum around 285 nm and a negative minimum around 248 nm, it was supposed that duplex structures existed in C-rich probes, and the probes were mixtures of both random coil structures and rigid duplex structures before binding to Ag^+, which is consistent with a previous report.[81] When Ag^+ was added, as the concentration of the Ag^+ increased, the positive maximum around 290 and 218 nm increased, and the negative minimum around 248 nm decreased, suggesting that the C-rich probe underwent a structure change from random coil single-stranded conformation to rigid duplex conformation, which was in good agreement with the DPI experiment results. It could also be observed from Figure 3B that the control DNA presented a CD spectrum with a positive maximum around 218 nm and a negative minimum around 248 nm, which was supposed to be the characteristic of the poly(A) sequence. After the addition of different concentrations of Ag^+, there was no noticeable change in this CD spectrum, indicating that Ag^+ did not bring about any effect on the conformational change of the control DNA.

Consequently, these CD experiments confirmed that Ag^+ interacted with C-rich ssDNA specifically and changed the structure of C-rich ssDNA from random coil single-stranded conformation to rigid duplex conformation.

Atomic Force Microscopy Characterization of Ag^+/probe/T_{30}/PEI Layer Growth. To further characterize the fabrication process of the biosensing layer and the interaction between the probe and Ag^+, atomic force microscopy (AFM) was used to directly determine the thickness of PEI layer, T_{30}/PEI layer, probe/T_{30}/PEI layer, and Ag^+/probe/T_{30}/PEI layer. Because our DPI experiments were conducted in a fluidic system and the immobilization of biosensing layer and the measurement of interaction between the probe and Ag^+ were achieved on line, AFM was utilized to measure dry interfaces off line in static condition, and the fabrication of the biosensing layer were conducted under ambient conditions. The surface environments of the chips were quite different between DPI and AFM, and thus ssDNA sequences on the two surfaces might adopt different conformations. Consequently, the AFM characterization could only give a general trend of the thickness value change. Figure S4 shows that the order of thickness was

dx.doi.org/10.1021/ac403992r | Anal. Chem. 2014, 86, 3849–3855

Ag^+/probe/T_{30}/PEI layer (32.2 nm), probe/T_{30}/PEI layer (31.3 nm), T_{30}/PEI layer (25.6 nm), and PEI layer (23.2 nm). The multilayer was thicker than that measured by DPI mainly due to the thickly deposited PEI layer. Thus, through analysis, the net thickness of T_{30} layer, probe layer, and Ag^+/probe layer were 2.4, 5.7, and 6.6 nm, respectively. The results were basically consistent with that of DPI, which further demonstrated the success of our new immobilization approach and the interaction of the probe with Ag^+.

Determination of Cysteine. Cysteine (Cys) plays a crucial role in human bodies,[82] thus the detection of Cys is important for the study of its activities. It is known that Cys has a strong reaction with Ag^+ and can capture Ag^+ from C−Ag^+−C complexes, resulting in the change of the structure of the C-rich ssDNA from rigid duplex conformation to random coil conformation. Thus, Cys could be detected in the similar way as Ag^+ using DPI. As is depicted in Figure S5, the changes of the mass (Figure S5A), thickness (Figure S5B), and density (Figure S5C) values at 450 s were plotted as a function of the corresponding concentration of Cys. The result showed that the changes of the mass, thickness, and density values were linear to the concentration of the Cys ranging from 500 nM to 10 μM. The linear equation could be fitted as mass (ng/mm^2) = 0.0388 − 0.0036c (Cys, μM) (R^2 = 0.996), thickness (nm) = 0.3748 − 0.0302c (Cys, μM) (R^2 = 0.993), and density (g/cm^3) = −0.0210 + 0.0017c (Cys, μM) (R^2 = 0.988) with a limit detection (3σ) of 100 nM, respectively.

To investigate the selectivity of this biosensor for Cys, 6 μM Cys and 6 μM of a mixture of 10 most common amino acids (Ala, Gln, Gly, Pro, His, Leu, Val, Phe, and Arg) were reacted with 3 μM Ag^+ for 30 min and then subjected to the DPI measurement. Figure S6 demonstrates that the mass (Figure S6A), thickness (Figure S6B), and density (Figure S6C) values for the solution of the mixture changed much less than that of Cys, suggesting a good selectivity for Cys.

CONCLUSION

This work investigated the interaction of C-rich ssDNA oligonucleotides with silver ions (Ag^+) in real time using the DPI technique. Ag^+ selectively bound to C−C mismatches and formed C−Ag^+−C complexes, inducing the structure of the C-rich DNA changing from random coil conformation to rigid double-stranded conformation, whereas the control DNA underwent no such changes, which was proved by CD spectroscopy and AFM characterization. The C-rich DNA was immobilized on an unmodified silicon oxynitride chip with a newly developed approach. After the addition of Ag^+, the real-time conformational changes of the DNA could be detected using DPI and explained in detail by use of mass, thickness, and density values. The results showed that as the concentration of Ag^+ increased, the mass and thickness values of the probe layer increased, while the density values decreased. In addition, the changes of the mass, thickness, and density values were proportional to the concentration of Ag^+ ranging from 10 nM to 8 μM, based on which a biosensor for Ag^+ was fabricated and utilized to detect real samples. This biosensor showed a high sensitivity and selectivity toward Ag^+ and avoided the interference from several other metal ions. What's more, as Cys could capture Ag^+ from the C−Ag^+−C complexes inducing the structure of the C-rich DNA changing back from rigid duplex conformation to random coil conformation, Cys could also be detected with DPI in the same way. The 10 most common amino acids did not produce any significant signals, suggesting a high selectivity of this biosensor for Cys.

The new approach used for immobilizing C-rich ssDNA on the chip surface improved the flexibility of the ssDNA. These probe ssDNA oligonucleotides oriented inclined and received little influence from the T_{30}/PEI layer, hence the interaction of the probe ssDNA with Ag^+ was more sensitive. This strategy paved a new avenue for studying the interaction of DNA with small molecules. It can be expected that DPI technique will be a potential means to explore and verify functional DNA interaction with different target molecules.

ASSOCIATED CONTENT

Supporting Information

Additional text describing mass, thickness, and density value changes of the probe/T_{30}/PEI layer and control DNA/T_{30}/PEI layer upon injection of different concentrations of Ag^+ or different concentrations of cysteine in presence of Ag^+; determination of the concentration of Ag^+ in drinking water samples; comparison of two methods used for creating the probe layer; selectivity of the biosensor for Ag^+ and cysteine independently; AFM images of PEI layer, T_{30}/PEI layer, probe/T_{30}/PEI layer and Ag^+/probe/T_{30}/PEI layer. This material is available free of charge via the Internet at http://pubs.acs.org.

AUTHOR INFORMATION

Corresponding Authors

*E-mail: (X.Y.) xryang@ciac.ac.cn. Fax: +86 431 85689278. Tel.: +86 431 85262056.
*E-mail: (F.Y.) fyang@ciac.ac.cn.

Notes

The authors declare no competing financial interest.

ACKNOWLEDGMENTS

This work was financially supported by the National Natural Science Foundation of China (no. 21175124), the National Key Basic Research Development Project of China (no. 2010CB933602), and Development Project of Science and Technology of Jilin Province (no. 20125090).

REFERENCES

(1) Sambhy, V.; MacBride, M. M.; Peterson, B. R.; Sen, A. *J. Am. Chem. Soc.* **2006**, *128*, 9798−9808.
(2) Bhardwaj, V. K.; Singh, N.; Hundal, M. S.; Hundal, G. *Tetrahedron* **2006**, *62*, 7878−7886.
(3) Fung, M. C.; Bowen, D. L. *J. Toxicol., Clin. Toxicol.* **1996**, *34*, 119−126.
(4) Alexander, J. W. *Surg. Infect.* **2009**, *10*, 289−292.
(5) Newman, M.; Kolecki, P. *Am. J. Emerg. Med.* **2001**, *19*, 525−526.
(6) Morgan, T. P.; Wood, C. M. *Environ. Toxicol. Chem.* **2004**, *23*, 1261−1267.
(7) Hogstrand, C.; Wood, C. M. *Environ. Toxicol. Chem.* **1998**, *17*, 547−561.
(8) Reinfelder, J. R; Chang, S. I. *Environ. Sci. Technol.* **1999**, *33*, 1860−1863.
(9) Hidalgo, E.; Dominguez, C. *Toxicol. Lett.* **1998**, *98*, 169−179.
(10) Poon, V. K. M.; Burd, A. *Burns* **2004**, *30*, 140−147.
(11) Torigoe, H.; Miyakawa, Y.; Nagasawa, N.; Kozasa, T.; Ono, A. *Nucleic Acids Symp. Ser.* **2006**, *50*, 225−226.
(12) Torigoe, H.; Kozasa, T.; Ono, A. *Nucleic Acids Symp. Ser.* **2006**, *50*, 89−90.
(13) Ono, A.; Miyake, Y. *Nucleic Acids Symp. Ser.* **2003**, *3*, 227−228.
(14) Shukla, S.; Sastry, M. *Nanoscale* **2009**, *1*, 122−127.

(15) Ono, A.; Cao, S.; Togashi, H.; Tashiro, M.; Fujimoto, T.; Machinami, T.; Oda, S.; Miyake, Y.; Okamoto, I.; Tanaka, Y. *Chem. Commun.* **2008**, *39*, 4825−4827.
(16) Li, T.; Shi, L.; Wang, E.; Dong, S. J. *Chem.—Eur. J.* **2009**, *15*, 3347−3350.
(17) Oh, J. H.; Lee, J. S. *Chem. Commun.* **2010**, *46*, 6382−6384.
(18) Kong, D. M.; Cai, L. L.; Shen, H. X. *Analyst* **2010**, *135*, 1253−1258.
(19) Li, B. L.; Du, Y.; Dong, S. J. *Anal. Chim. Acta* **2009**, *644*, 78−82.
(20) Wen, Y. Q.; Xing, F. F.; He, S. J.; Song, S. P.; Wang, L. H.; Long, Y. T.; Li, D.; Fan, C. H. *Chem. Commun.* **2010**, *46*, 2596−2598.
(21) Man, B. Y. W.; Chan, D. S. H.; Yang, H.; Ang, S. W.; Yang, F.; Yan, S. C.; Ho, C. M.; Wu, P.; Che, C. M.; Leung, C. H.; Ma, D. L. *Chem. Commun.* **2010**, *46*, 8534−8536.
(22) Lin, Y. H.; Tseng, W. L. *Chem. Commun.* **2009**, *43*, 6619−6621.
(23) Zhao, C.; Qu, K. G.; Song, Y. J.; Xu, C.; Ren, J. S.; Qu, X. G. *Chem.—Eur. J.* **2010**, *16*, 8147−8154.
(24) Freeman, N. J.; Peel, L. L.; Swann, M. J.; Cross, G. H.; Reeves, A.; Brand, S.; Lu, J. R. *J. Phys.: Condens. Matter* **2004**, *16*, S2493−S2496.
(25) Biehle, S. J.; Carrozzella, J.; Shukla, R.; Popplewell, J.; Swann, M.; Freeman, N.; Clark, J. F. *Biochim. Biophys. Acta* **2004**, *1689*, 244−251.
(26) Swann, M. J.; Peel, L. L.; Carrington, S.; Freeman, N. J. *Anal. Biochem.* **2004**, *329*, 190−198.
(27) Lu, J. R.; Swann, M. J.; Peel, L. L.; Freeman, N. J. *Langmuir* **2004**, *20*, 1827−1832.
(28) Sonesson, A. W.; Callisen, T. H.; Brismar, H.; Elofsson, U. M. *Colloids Surf., B* **2007**, *54*, 236−240.
(29) Sonesson, A. W.; Callisen, T. H.; Brismar, H.; Elofsson, U. M. *Colloids Surf., B* **2008**, *61*, 208−215.
(30) Lin, S.; Lee, C. K.; Wang, Y. M.; Huang, L. S.; Lin, Y. H.; Lee, S. Y.; Sheu, B. C.; Hsu, S. M. *Biosens. Bioelectron.* **2006**, *22*, 323−327.
(31) Sheu, B. C.; Lin, Y. H.; Lin, C. C.; Lee, A. S. Y.; Chang, W. C.; Wu, J. H.; Tsai, J. C.; Lin, S. M. *Biosens. Bioelectron.* **2010**, *26*, 822−827.
(32) Daghestani, H. N.; Fernig, D. G.; Day, B. W. *Biosens. Bioelectron.* **2009**, *25*, 136−141.
(33) Gupta, S.; Modak, R.; Surolia, N.; Surolia, A. *Biochem. Biophys. Res. Commun.* **2009**, *380*, 763−768.
(34) Lundin, M.; Sandberg, T.; Caldwell, K. D.; Blomberg, E. *J. Colloid Interface Sci.* **2009**, *336*, 30−39.
(35) Tan, O.; Cross, G. H. *Phys. Rev. E.* **2009**, *79*, 021703−021713.
(36) Boudjemline, A.; Saridakis, E.; Swann, M. J.; Govada, L.; Mavridis, I. M.; Chayen, N. E. *Anal. Chem.* **2011**, *83*, 7881−7887.
(37) Song, H. Y.; Zhou, X. D.; Hobley, J.; Su, X. D. *Langmuir* **2012**, *28*, 997−1004.
(38) Zhao, X. B.; Pan, F.; Cowsill, B.; Lu, J. R. *Langmuir* **2011**, *27*, 7654−7662.
(39) Cowsill, B. J.; Coffey, P. D.; Yaseen, M.; Waigh, T. A.; Freeman, N. J.; Lu, J. R. *Soft Matter* **2011**, *7*, 7223−7230.
(40) Zhai, J. L.; Wooster, T. J.; Hoffmann, S. V.; Lee, T. H.; Augustin, M. A.; Aguilar, M. I. *Langmuir* **2011**, *27*, 9227−9236.
(41) Lane, T. J.; Fletcher, W. R.; Gormally, M. V.; Johal, M. S. *Langmuir* **2008**, *24*, 10633−10636.
(42) Feldötö, Z.; Varga, I.; Blomberg, E. *Langmuir* **2010**, *26*, 17048−17057.
(43) Westwood, M.; Noel, T. R.; Parker, R. *Biomacromolecules* **2011**, *12*, 359−369.
(44) Lundin, M.; Solaqa, F.; Thormann, E.; Macakova, L.; Blomberg, E. *Langmuir* **2011**, *27*, 7537−7548.
(45) Karabulut, E.; Wagberg, L. *Soft Matter* **2011**, *7*, 3467−3474.
(46) Terry, C. J.; Popplewell, J. F.; Swann, M. J.; Freeman, N. J.; Fernig, D. G. *Biosens. Bioelectron.* **2006**, *22*, 627−632.
(47) Mashaghi, A.; Swann, M.; Popplewell, J.; Textor, M.; Reimhult, E. *Anal. Chem.* **2008**, *80*, 3666−3676.
(48) Sanghera, N.; Swann, M. J.; Ronan, G.; Pinheiro, T. J. T. *Biochim. Biophys. Acta* **2009**, *1788*, 2245−2251.
(49) Lee, T. H.; Heng, C.; Swann, M. J.; Gehman, J. D.; Separovic, F.; Aguilar, M. I. *Biochim. Biophys. Acta* **2010**, *1798*, 1977−1986.
(50) Nielsen, S. B.; Otzen, D. E. *J. Colloid Interface Sci.* **2010**, *345*, 248−256.
(51) Baumann, M. K.; Swann, M. J.; Textor, M.; Reimhult, E. *Anal. Chem.* **2011**, *83*, 6267−6274.
(52) Blum, S. R.; Peel, L. L.; Ruggiero, F.; Freeman, N. J. *Anal. Biochem.* **2006**, *352*, 252−259.
(53) Lin, S. M.; Lee, C. K.; Lin, Y. H.; Lee, S. Y.; Sheu, B. C.; Tsai, J. C.; Hsu, S. M. *Biosens. Bioelectron.* **2006**, *22*, 715−721.
(54) Karim, K.; Taylor, J. D.; Cullen, D. C. *Anal. Chem.* **2007**, *79*, 3023−3031.
(55) Thompsett, A. R.; Brown, D. R. *Biochim. Biophys. Acta* **2007**, *1774*, 920−927.
(56) Berney, H.; Oliver, K. *Biosens. Bioelectron.* **2005**, *21*, 618−626.
(57) Lillis, B.; Manning, M.; Berney, H.; Hurley, E.; Mathewson, A.; Sheehan, M. M. *Biosens. Bioelectron.* **2006**, *21*, 1459−1467.
(58) Lee, L.; Johnston, A. P. R.; Caruso, F. *Biomacromolecules* **2008**, *9*, 3070−3078.
(59) Kato, N.; Lee, L.; Chandrawati, R.; Johnston, A. P. R.; Caruso, F. *J. Phys. Chem. C.* **2009**, *113*, 21185−21195.
(60) Ferreira, V. C.; Melato, A. I.; Silva, A. F.; Abrantes, L. M. *Electrochem. Commun.* **2011**, *13*, 993−996.
(61) Nowicka, A. M.; Kowalczyk, A.; Sek, S.; Stojek, Z. *Anal. Chem.* **2013**, *85*, 355−361.
(62) Masuda, T.; Sonsudin, F.; Singh, P. R.; Naohara, H.; Uosaki, K. *J. Phys. Chem. C.* **2013**, *117*, 15704−15709.
(63) Song, H. Y.; Sun, W.; Prabhakar, S.; Aung, K. M. M.; Su, X. D. *Anal. Biochem.* **2013**, *433*, 121−128.
(64) Özalp, V. C. *Anal. Bioanal. Chem.* **2012**, *402*, 799−804.
(65) Wang, J.; Xu, X. W.; Zhang, Z. X.; Yang, F.; Yang, X. R. *Anal. Chem.* **2009**, *81*, 4914−4921.
(66) Wang, J.; Coffey, P. D.; Swann, M. J.; Yang, F.; Lu, J. R.; Yang, X. R. *Anal. Chem.* **2010**, *82*, 5455−54622.
(67) Wang, Y.; Zheng, Y.; Yang, F.; Yang, X. R. *Chem. Commun.* **2012**, *48*, 2873−2875.
(68) Gooding, J. J. *Electroanalysis* **2002**, *14*, 1149−1156.
(69) Soto, C. M.; Patterson, C. H.; Charles, P. T.; Martin, B. D.; Spector, M. S. *Biotechnol. Bioeng.* **2005**, *92*, 934−942.
(70) Zhang, J.; Chua, L. S.; Lynn, D. M. *Langmuir* **2004**, *20*, 8015−8021.
(71) Gong, H.; Li, X. H. *Analyst* **2011**, *136*, 2242−2246.
(72) Xie, W. Y.; Huang, W. T.; Li, N. B.; Luo, H. Q. *Chem. Commun.* **2012**, *48*, 82−84.
(73) Chang, C. C.; Lin, S. H.; Wei, S. C.; Chu-Su, Y.; Lin, C. W. *Anal. Bioanal. Chem.* **2012**, *402*, 2827−2835.
(74) Johnston, A. P. R; Read, E. S.; Caruso, F. *Nano Lett.* **2005**, *5*, 953−956.
(75) Murphy, M. C.; Rasnik, I.; Cheng, W.; Lohman, T. M.; Ha, T. *Biophys. J.* **2004**, *86*, 2530−2537.
(76) Papadakis, G.; Tsortos, A.; Bender, F.; Ferapontova, E. E.; Gizeli, E. *Anal. Chem.* **2012**, *84*, 1854−1861.
(77) Kypr, J.; Kejnovska, I.; Renciuk, D.; Vorlıckova, M. *Nucleic Acids Res.* **2009**, *37*, 1713−1725.
(78) Megger, D. A.; Müller, J. *Nucleosides, Nucleotides Nucleic Acids* **2010**, *29*, 27−38.
(79) Nakano, S.; Wu, L.; Oka, H.; Karimata, H. T.; Kirihata, T.; Sato, Y.; Fujii, S.; Sakai, H.; Kuwahara, M.; Sawai, H.; Sugimoto, N. *Mol. BioSyst* **2008**, *4*, 579−588.
(80) Nakano, M.; Moody, E. M.; Liang, J.; Bevilacqua, P. C. *Biochemistry* **2002**, *41*, 14281−14292.
(81) Wei, H.; Li, B. L.; Li, J.; Wang, E. K.; Dong, S. J. *Chem. Commun.* **2007**, *36*, 3735−3737.
(82) Goodman, M. T.; McDuffie, K.; Hernandez, B.; Wilkens, L. R.; Selhub, J. *Cancer* **2000**, *89*, 376−382.